



Design a long-range near infrared LiDAR imaging system for security and surveillance applications

Y. Chalapathi Rao¹ · L. Srinivasa Rao² ·
G. Ramesh Chandra³ · M. Satyanarayana¹

Received: 10 June 2024 / Accepted: 7 September 2024
© The Author(s), under exclusive licence to The Optical Society of India 2024

Abstract In this paper a review on the state of art on the imaging lidar system useful for security and surveillance applications is discussed. An imaging lidar system design and developed in house is also described. The theoretical approach of the system developed in house is presented. Based on the approach the technical parameters of a proposed long-range lidar system have been finalized and the designed specifications of various components/sub-systems were also derived. A laser transmitter, which operates at the wavelength of 1064 nm in the NIR region is used in the system. An analysis of the system is presented describing the expected values of received energy (E_r) / power (P_r) and the SNR of the system have been determined for various values of co-efficient reflectivity and size of the target. Three factors that are affecting the imaging systems have been discussed namely i. resolution requirements in terms of pixels of detector, ii. atmospheric turbulence in terms of index of refraction due to time-varying thermal inhomogeneities, and iii. atmospheric attenuation, which includes absorption and scattering. The use of range gating technique was described, which enables the imaging of the target at a fixed range, while minimizing the atmospheric effects on the image quality. The range gating substantially improves the SNR of the imaging system. The lidar system can be operated in both day and night conditions, even though its use

is essentially meant for nighttime conditions as required for security and surveillance.

Keywords Atmospheric effects · LIDAR · Range gating · SNR · Security and surveillance

Introduction

Homeland security, night surveillance, sea search, rescue & maritime patrol missions, border security, police law enforcement, etc., pose several challenges for the imaging system required for these applications. Such systems must work under low light or pitch dark, low visibility, and adverse atmospheric conditions [1–5]. Also, the imagery systems are deeply impacted by atmospheric possessions, particularly rain, fog and haze which drastically reduce the detection range, image contrast, and resolution. They have to provide the long-range capability to detect and identify the targets under different environments. Usually, the sensors are used to detect and identify different possible targets such as persons, vehicles and ships [4, 5].

Customary night vision systems let operators surreptitiously track and showcase the targets at long distance. These night vision sensors are essentially of passive type. They make use of the moonlight or starlight background or the thermal features of the target and the scene [6, 7]. Image intensifiers are used in these systems designed for the short-range night vision military applications. For long-range, military forces use high resolved and reliable thermal images based on the infrared radiation principle. But, even the advanced thermal imaging systems have definite vital shortfalls as follows:

- The difficulty in recognizing objects at long range

✉ Y. Chalapathi Rao
chalu.8421@gmail.com

¹ Department of ECE, VNRVJIET, Hyderabad,
Telangana 500090, India

² Department of Physics, VNRVJIET, Hyderabad,
Telangana 500090, India

³ Department of CSE, VNRVJIET, Hyderabad,
Telangana 500090, India

- Diminished performance in rain, snow and fog
- Impossible to see through window panes

So as to resolve the problems associated with the above passive systems, in recent days, active laser night vision technologies have been used for homeland security and other surveillance applications with many advantages [4, 5]. Gabriel Popa, et al. have described Long Range LiDAR system for sensing distance objects for vehicle safety application experimentally [8]. The experimental findings emphasize the sensitivity of the sensor to fake targets and objects, which are important for evaluating long-range LiDAR capabilities in sensing safety distance for vehicles. Peng-Yu Jiang, et al. proposed a Long-range 3D imaging system through atmospheric obscurants using array-based single-photon LiDAR [9]. This system is capable of 3D imaging through atmospheric obscurants including fog, haze and smoke. Also, the system is used for practical applications of target recognition and vehicle navigation in challenging weather conditions. Ahui Hou, et al. proposed a LiDAR system for target ranging and tracking by four-quadrant photon counting. This method includes signal processing, extraction of pixel intensity, and positioning for targets. It provides positioning and tracking of small moving targets over long distances [10].

Background Active Imaging systems intended for security and surveillance applications make use of laser as the radiation for illuminating the target and measure the reflected/scattered intensity returned from the target by employing suitable optical receivers. Such a system is generally called as lidar system or optical radar which is analogous to radar working in the RF region [4, 5]. An imaging lidar system essentially consists of a transmitter, a receiver and a detector followed by the data acquisition, image processing and recording systems. A laser source of appropriate wavelength, power, pulse width, pulse repetition frequency etc. is used in the transmitter along with a suitable beam expander / collimator optics to expand the beam to the size as needed for illuminating the target scene. The reflected / scattered intensity is collected by an optical telescope and focused on a two-dimensional area photodetector. The output of the two-dimensional area detector is used to generate the raw image of the target by the frame grabber, on the other hand, the distance of the target from the trans-receiver is also obtained at the same time by the time of flight (TOF) measurement. The raw image of the target is recorded and subjected to image processing for improving the quality of the image with the expected contrast and resolutions. The processed images of the target are used for detection /recognition/identification of the target as per the requirements and transmitted through internet/cable to the remotely located control and command station for real time security and surveillance applications [1–5]. The laser imaging system can be operated both in the non-gated and range-gated modes depending

upon the requirement. The system can be operated in the passive mode by using a simple conventional low-light-level camera, which depend on the natural lighting sources of illumination (example: daylight, twilight conditions etc) to obtain the target image. On the other hand, the pulsed laser light illuminates the target in the active mode.

The camera system is gated to switch ‘ON’ such that it receives and amplifies the reflected light from the target. A narrow band filter of the wavelength (≈ 1064 nm) and the reasonably very short ‘ON’ time of the camera initially collect the inadequate light for the image signals. However, by varying the delay time between the transmitting laser pulse and the ‘ON’ time of the camera, the minimum range of the target can be varied harmoniously. This allows elimination of the effects of rain, smoke or haze on the backscattered signal from the target. So, the image quality gets improved. The ‘ON’ time of the camera establish the depth of field. The range-gated laser imaging system can also be operated in the normal non-gated mode, if required [4, 11].

Design principle

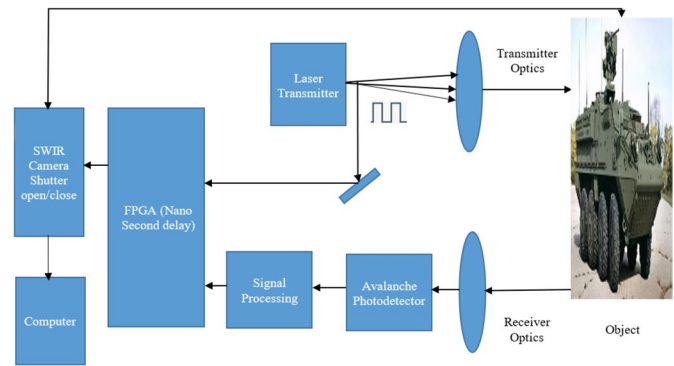
Design of long range active imaging system

This Paper describes the design, development, and analysis of a long range LIDAR system, which can be used for many applications in security and surveillance. The laser operates in the infrared region and as such can't be visually seen or observed at the location of the target and jammed unlike in the case of radar imaging [12]. The laser transmitter parameters can be selected based on the target range, target size, target reflectivity etc. and also on the prevailing atmospheric conditions. It makes use of a short wave infrared (SWIR) camera with suitable front lens to receive the two-dimensional intensity profile and helps to produce the raw image for further processing and generates a quality image for recording and analysis. The resolution and contrast of the target can be greatly improved by using conventional image processing methods. The system will have the capability to image the target scenes up to at least 2 km, depending upon the target reflectivity even under adverse atmospheric conditions, using the time gating technique additionally. The system can be operated both day and night conditions, even though its use is essentially nighttime conditions as required for security and surveillance in defence.

System description

This system consists of mainly a laser transmitter, a receiver, data acquisition, display, and recording system. The block diagram of the proposed system is shown in Fig. 1.

Fig. 1 Schematic diagram of proposed Long-range LIDAR imaging system



Laser source Diode-Pumped Solid-State Pulsed Nd:YAG Laser (Q-Switched DPSSL Actively & Passively Q-Switched; pulse width 10 ns and Average power 100 mW) with multi-wavelength emission 1064 nm, 532 nm, 355 nm, 266 nm is used. However, we operate at 1064 nm for day and night use.. The laser operates in pulsed mode with a pulse width < 10 ns, energy 2 mJ, and at a pulse repetition frequency (PRF) 50Hz. One of the important parameters for selecting a laser source is the operational wavelength. The lidar operation is to be used in security and surveillance applications; hence the operational wavelength would be in the infrared region. So that it can be either in the NIR or MIR regions due to practical availability of lasers in terms of suitable wavelength, simplicity in operation (no need of cooling), and relatively low cost. Also, the laser should be ruggedized and suitable for field views. Yet, other important specifications like peak and average powers, pulse duration, pulse repetition frequency, and reliability of the emitted beam are also the important aspects for designing the lidar system. So far, the Nd: YAG laser in the category of solid-state laser is dexterous of producing extraordinary peak power, high PRF, and narrow pulse width of laser (< 10 ns). It's a very rugged, reliable proven laser system used for many LIDAR applications with long life [4–6]. In view of these merits of Nd: YAG laser and its technical suitability and availability, it is decided to propose the use of Nd: YAG laser, which emits fundamental wavelength of 1064 nm in NIR region. Why 1064 nm wavelength of Laser can be used in our system? The 1064 nm wavelength is considered eye-safe, meaning it poses minimal risk of eye damage compared to shorter wavelengths. All personnel in the area must wear laser goggles during operation of the laser. This protective eyewear must be effective at the wavelength 1064 nm generated by the laser. It has good penetration capabilities through optically dense media like fog, smoke, and rain conditions. The near-infrared (NIR) region experiences less scattering in the atmosphere, leading to improved signal-to-noise ratio (SNR) and better imaging quality.

Transmitting optics Before transmitting the laser towards the target, it is necessary to expand and collimate the beam

suitably to illuminate the target area at the range prescribed. The laser source selected for the operation has a divergence of 0.6 m rad as given in the specifications of the same. We have selected a beam expander and a collimator which facilitates to expand, collimate and diverge also as per the requirements for imaging of the targets of different sizes, shapes, and with different reflectivity characteristics. It may be noted that the selected wavelength of 1064 nm can pass through the glass windows also, unlike passive thermal imagers when it is required the image of the targets situated inside the trucks and cars, etc. The transmitting optics is designed to provide a collimated beam of 10 mRad, and also a diverging beam to provide an illuminated spot of diameter 20 m at the range of 2 Km. The beam divergence analysis of the lidar system to optimize the detection range was reported recently by Duck-Lae Kim et al [13].

Receiver optics The receiver optics is intended to collect the reflected/ scattered laser signal returning from the target in the direction of the transmitter, which is co-located with the transmitter at same workstation. Considering the requirements of the target imaging, it is decided to use telescope optics of circular aperture with diameter 100 mm as described by Ge et al [14].

Detector module The selection of a photodetector depends on its characteristics such as quantum efficiency, current gain, dark current, spectral response, and frequency response. Generally, the wavelength of the illuminating signal is the key factor in selection of photodetector to be used in the application. Also, for imaging systems, we need to use a 2D area detector of suitable size and required number of pixels depending upon the spatial resolution of the target required. The receiver optics collects the signal from the targets and focuses on the detector module. Silicon-based detectors are more suitable for detecting the reflected signals from the target at 1064 nm. We make use of a 2D silicon area detector for imaging the target from the received signals. (Selection of the Si- detector is to be finalized- Size and no. pixels, etc. Avalanche photodetector (APD) module for measurement of the range (optional). As mentioned

earlier, a separate channel is used for measuring the range of the target by an Avalanche photodetector module. For this purpose, a part of the received signal can be received by the telescope, and then focus on the APD detector. An optical beam splitter is used for providing the signal onto the Avalanche photodetector module. The current output of the APD is amplified and digitized. A range gating unit is designed and developed for sampling the signal to measure the amplitude and timing of the signal at various range bins. From these data, the range of the target will be obtained by using the time of flight principle [15]. The range sensor plays a crucial role in determining the range of target by emitting laser pulses and detecting the reflected signals. The sensor determines the time-of-flight (ToF) of these pulses, which is then used to calculate the precise distance between the LiDAR system and various reflection points from different targets in the line of sight. In FPGA (Field-Programmable Gate Array) designs, achieving precise timing delays in the nanosecond range is indeed possible. FPGAs are semiconductor devices that can be programmed and reconfigured to implement various digital logic functions and custom hardware designs. They offer a high degree of flexibility, making them well-suited for applications that require precise timing control, such as communication protocols, signal processing, and other real-time applications.

Counter-based delay One straightforward method is to use a counter to introduce a delay. For example, if you know the FPGA clock frequency and the desired delay in nanoseconds, you can calculate the number of clock cycles needed to achieve that delay and use a counter to count those cycles before passing the signal to the output.

Data acquisition and processing

The output of the SWIR camera gives an image of the target. The image obtained from the SWIR camera is recorded in a computer system using a frame grabber card installed in the computer [4, 7]. Frame grabber is a digital device that grabs distinct stills of digital frames thru the analog image signals or a digital image streams. The image of the target scene is recorded after preprocessing in a single board computer equipped with a Frame Grabber card for real-time analysis and for offline storage. The raw image of the target is tagged with the range data obtained from the time of flight (TOF) measurement to obtain the direct image of the target scene. The raw image of the target scene is subjected to image processing methods (direct image processing) to enhance the image contrast and quality with good resolution. The final image can be reconstructed as a raw image by the Computer software and displayed on the screen (monitor) [4, 5].

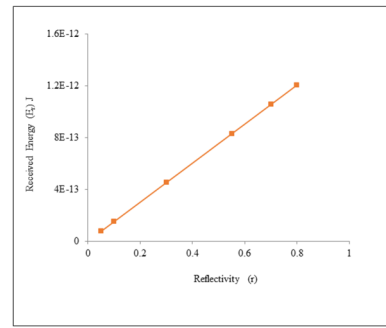


Fig. 2 Received energy (E_r) as a function of reflectivity(r) of the target

System design and analysis

The design techniques of a system are analyzed to estimate the expected received signals from different targets and sources of noise in the system. The range capability of a system is estimated by considering the SNR under different conditions [4].

The lidar equation

The fundamental lidar equation for the received laser energy E_r from a reflecting target is expressed as follows [4, 16]:

$$E_r = E_t \eta_T \eta_R r \left(\frac{AT^2}{R^2} \right) \quad (1)$$

Where, E_t is the transmitted energy, r is the reflectivity of the target, R is the range of the target, T is transmittivity of the atmosphere, η_T is optical efficiency of the transmitter system, η_R is optical efficiency of the receiver system, and A is area of the telescope.

Usually, the signal reflectivity of the specific target can be influenced by the wavelength of laser, aspect angle, type of the target, and its surface finish. Background vegetation and top soil show good reflectivity (10–40 %) in the NIR; we may expect adequate reflectivity about 15% in the proposed system. In this regard we have shown below the expected energy and power data from the target for different reflectivity values from 5–80 % for a target at 2 km range from the transmitter.

The following are the parameters of the proposed system while calculating the Energy and power values.

Laser Transmitted Energy = 2 mJ

Laser Pulse Width = 10 ns

Laser PRF = 50 Hz

Transmitted Wavelength = 1064 nm

Assumed atmospheric transmittance = 0.6

Area of the Telescope = 0.00785 m².

Received energy and received power for different reflectivity of the target are calculated. The pertinent data is presented in Table 1. Figure 2 shows received energy (E_r) as a function of reflectivity(r) of the target. The received energy and power are observed to increase gradually as the reflectivity of the target increases.

Here, we have to note the following things:

- The energy and peak power data are applicable for the camera sensor used for imaging and APD sensor used for range measurement respectively in the long range LIDAR system.
- The signal to noise ratio values are calculated for the imaging and range finding channels accordingly.
- The long range imaging LIDAR system is used for night time imaging applications and the APD channel is meant for range finding simultaneously.
- The SNR value for the IR sensitive camera is typically 48 dB or 251.

Signal and noise estimates

Noise

The lidar systems play vital role in the 3-D imaging sector, owing to its distinctive characteristics like good resolution for long-range and extensive scanning of the target. One of the most essential parameters of lidar is the signal-to-noise ratio (SNR). The SNR not only shows the capability in target imaging, but also gives some inputs in the design of the lidar. As distance of the target increases the SNR decreases, then the retrieval capacity of the lidar becomes feeble [4, 7, 12]. Yet, there is no a standard technical method to determine the SNR of a lidar in practice. However, the suitable method is adopted by considering the factors that affect the lidar system. The factors include a variety of technical parameters as follows: Range of the target object (R), wavelength of pulsed laser ($\lambda \approx 1064$ nm), Pulse width (b), Pulse repetition frequency (PRF), intensity of the transmitted signal (Tx), Signal loss, Signal scattering, Diameter of

illumination on the target (D), Target reflectivity (r), Signal noise, Intensity of received signal (Rx), Area of the receiving optics (A), Sensitivity of photodetector (s), Integration time (ti), and data processing. The distortion or disturbance in the laser pulse emitted by the laser source is called signal noise. The signal noise is of three types.

Background noise due to the effect of solar light. There may be overlapping of the signal with the light emitted by other light sources in the surroundings. Also, the light emitted through the space, such as sunlight (at daytime), moonlight (at night time), planetary light, etc., can induce the noise in the Laser signal between the transmission and reflection. This is minimized by arranging an optical filter in the receiver [17].

Dark current noise due to current flow in the photodetector in the absence of light illumination. This type of noise is the random in nature. Thermal noise and dark current noise are fundamental sources of noise in a photodiode. The load resistor of photo diode is responsible for the thermal noise. The spectral density of thermal noise does not dependent on the frequency, thus commonly it is referred to as a white noise or Johnson noise. By increasing the value of a load resistance (RL), hence the RC constant increases, then the bandwidth of receiver becomes narrow. Generally, $RL \approx 50 \Omega$ is used as a standard load resistance in high speed optical receivers [18].

Quantum noise (shot noise) is the signal-induced noise by the Laser source. Quantum noise (or shot noise) generates thru the statistic nature of the photodetector. E.g., assuming optical power of $1 \mu W$ and operational wavelength of 1064 nm illuminated on a photodiode, and then about 5.3 trillion photons per sec would focus on the photodiode statistically. Usually, quantum noise is directly proportional to the square root of the intensity of the signal. The intensity of the received signal by the photodetector can be determined by

$$I = \frac{Nhc}{A\lambda} \tag{2}$$

where, N is number of photons, h is Planck’s constant, c is velocity of the light, A is incident area of the photodetector and λ is wavelength of the laser source.

SNR estimation for the LIDAR system

Background noise is a prime adversary parameter to all types of lidar systems, it can never be eliminated. However, several methods are available in practice to eliminate the noise substantially by using narrow bandpass filters [17]. The narrow band bandpass filters (bandwidth <10nm) have been employing in the lidar applications. These filters are very sensitive to change of temperature of the environment, and also they have narrow acceptance angle.

Table 1 Received energy and power for different reflectivity of the target

Reflectivity of the target (r)	Received energy (E_r) J	Received power (P_r) mW
0.05	7.536E-14	0.07536
0.1	1.5072E-13	0.15072
0.3	4.5216E-13	0.45216
0.55	8.2896E-13	0.82896
0.7	1.05504E-12	1.05504
0.8	1.20576E-12	1.20576

We have calculated the SNR by using the following formulas [19]:

$$SNR = \frac{S}{\sqrt{(S + B + Y)}} \tag{3}$$

$$SNR = \frac{I_s}{I_k} = \frac{I_s}{\sqrt{2e\Delta f(I_s + I_b + I_d)}} \tag{4}$$

Where I_b is back ground radiance, I_d is dark current noise, I_k is total noise current of the system at the APD, I_s received signal current, and e is electron charge.

Responsivity = 24 A/W

Received signal current = [Responsivity × Received Signal power]

Δf =Electrical System bandwidth =1 M Hz

I_b = 3.69 × 10-16 A (Night time)

I_b =29.52 × 10-10 A (Day time)

I_d = 5 × 10-9 A

Compared to the received signal current, the dark current noise and back ground radiance is negligible in both day and night conditions. It can be seen that without any time integration of the received signals from the target even with single pulse measurement. The signal to noise ratio is quite adequate for accurate measurement of the target.

SNR is computed as a function of received power. Figure 3. shows SNR as a function of received power. The pertinent data is shown in Table 2.

Role of the ambient condition on the imaging system

Image quality requirements

The range capability of the imaging o system defines in terms of recognition, identification of the target. It is primarily based on the number and size of pixels of the camera and the SNR ratio related to the receiver system. The resolution of the camera depends on size of the pixels. By increasing the number of pixels with in the specified size of

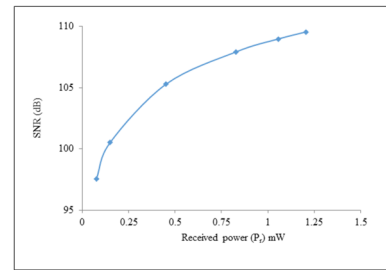


Fig. 3 Signal to Noise Ratio (SNR) as a function of Received Power

the pixel the target can pass through the stages of the detection, recognition, and identification. It is generally known that recognition, identification require 100–200 pixels and 200–400 pixels respectively.

Laser beam transmission through atmosphere

Transmission of laser beam of the transmitter through the atmosphere is effected by turbulence, scattering and attenuation of the medium. In lower atmosphere, particularly in the boundary layer, the effect is manifested mostly by aerosol scattering and turbulent medium. The contributions of both aerosol scattering and the turbulence are highly variable in space and time. The aerosol scattering depends upon the size, refractive index and the number density of the aerosol in the atmosphere, though complex it can be estimated. More importantly the effect of turbulence on the propagation of laser beam is severe by causing scintillation, beam dancing, beam spreading and spectral broadening. The atmospheric turbulence is caused by the propagation of thermal currents from the ground through the lower atmosphere. The temperature in the form of eddys is caused by the heating of ground and reemission of the radiation in thermal region. This causes the variation of refractive index of the medium and their by modifies the propagation of laser beam. The refractive index structure parameter (C_n^2) is an important factor to understand the atmospheric turbulence. C_n^2 value can be measured by using mainly three methods i. the gradient method of Zamek et al. [20], ii. Deep learning method [21], and iii. Temperature gradient method. The prediction

Table 2 Calculated SNR from Received power at different reflectivity values

Received power (P_r) mW	Received current(I_s) A	Total noise current (I_k) A	SNR	SNR in dB
0.07536	0.00180864	2.40575E-08	75179.78	97.52202
0.15072	0.00361728	3.40225E-08	106320.3	100.5323
0.45216	0.01085184	5.89287E-08	184152.1	105.3035
0.82896	0.01989504	7.97898E-08	249343.1	107.9359
1.05504	0.02532096	9.0015E-08	281297	108.9833
1.20576	0.02893824	9.62301E-08	300719.1	109.5632

and correction of the C_n^2 values can be done by using the neural network. By applying the CNN architecture the long-range images and scintillator values of the same location are required. In the deep learning model, the following formula is used [22].

$$C_n^2 = \left[\frac{PFV^2 X D^{\frac{1}{3}}}{LXP} \right] X \left[\frac{var(I)}{conv(I)} \right] \quad (5)$$

Where ‘PFV’ is the pixel field of view in radians, ‘D’ is the diameter of the lens aperture, ‘L’ is the distance from the camera to the target, ‘P’ is the turbulence constant parameter, ‘Var(I)’ is image variance, and ‘Conv(I)’ is a convoluted image. These parameters affect the quality of image by choosing the arbitrary locations of the image pixel randomly. There are some software methods to quantify such effects for good image quality [21–23].

Atmospheric attenuation

The laser wavelength is attenuated by the two component atmosphere consist of aerosol and gas molecules up to lower stratosphere altitudes. The transmission of laser of a ground based lidar imaging system is attenuated due to scattering and absorption by aerosols and molecule, fog, rain and smoke etc. The absorption caused by the above factors reduces the intensity of light reaching the target and their by SNR ratio of the imaging system. So as to mitigate atmospheric conditions on the transmitted laser beam, and there by enhance an image quality, it is envisaged to apply the range/time gating technique. It involves basically providing a suitable delay between the transmitter from the laser head and the opening of the receiver. The relative delay between the laser pulse and the starting of the receiver system helps to enhance the SNR and hence related image quality.

Target detection and range

Range gating methodology

The proposed system design contains range gating technology, which gains an important and useful method, particularly for long-range surveillance requirements. Active imaging incorporating the range gating technology is the most powerful and versatile method [24]. It is also known as time gating technology, which is illustrated in Fig. 4.

The range gating method operating in the NIR/SWIR contains two basic components: first one is pulsed laser source, and second one specifically designed camera that functions at high speed. The laser pulse is transmitted towards the target for illuminating the target and the SWIR camera with range gating facility is used to detect the reflected light. In

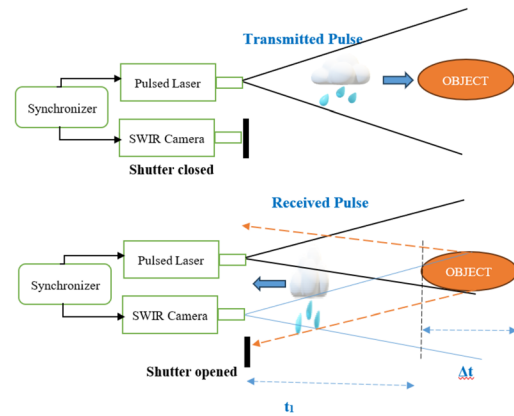


Fig. 4 Optical schematic of range-gating methodology

order to image only identify the target while minimizing the background noise the emission timing of the laser pulse is synchronized with the time of opening and closing of shutter of the camera. A synchronous reference pulse from the laser source is used to gate the time of exposure of the target by the camera is used per precisely imaging the target [25]. The duration of this gate opening is matched with the laser pulse duration which is of the order of few nanoseconds. This facilitates the avoidants of atmospheric effects such as rain, fog, smoke, etc. on the image quality, resolution, etc.

Detection of multiple targets

It is possible to detect and determine the range of all the targets in the path of the laser pulse limited to the maximum range capability of the system, when multiple targets are present at different ranges. However this is possible only to the extent that the beam is not fully obscured by the limited target and passes to reach the target at a greater distance corresponding to a later time. This process continues the next target and so on till signal to noise ratio of the reflected signal is sufficient from the farthest target. In this case the return signal contains reflected pulses corresponding to the target at varying distances with time delays related to their range and applicable for hard targets which are fully opaque. In the case of obscurations such as foliage or camouflaged target the lidar return signal will show up multiple return pulses corresponding to the pulse reaching next target through targets like trees and branches [24–26].

Table 3 shows the received energy, power and SNR for different sizes of the objects. We have assumed that the reflectivity of the object is uniformly about 0.5. However, in reality the reflectivity of the object may changes across its surface at different regions. The intensity reflected from various areas of the object can be normalized by applying the histogram equalization method [27], and the high contrast image with good resolution is obtained with

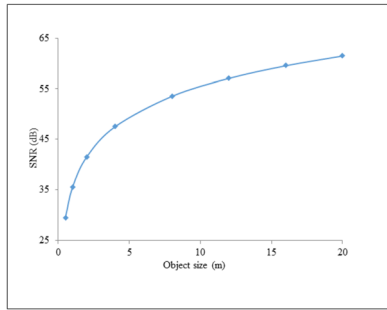


Fig. 5 Variation of SNR as a function of object size

Table 3 Received energy, power and SNR for different sizes of the objects with 50% reflectivity

Size of the object (meter)	E_r (J)	P_r (W)	SNR in dB
20	1.884E-16	1.884E-08	61.50142
16	1.20576E-16	1.20576E-08	59.56322
12	6.7824E-17	6.7824E-09	57.06445
8	3.0144E-17	3.0144E-09	53.54262
4	7.536E-18	7.536E-10	47.52202
2	1.884E-18	1.884E-10	41.50142

help of the licensed software tools such as mat lab, python etc. The calculated SNR for various sizes of the object is observed to be more than 29 dB as shown in Fig. 5, which is sufficient enough for lidar imaging up to 2 km [4, 5].

Laser range finder

The accurate range of the target from the lidar is to measure with good accuracy. It is proposed to design and develop a laser range finder in addition to measurement of range to be obtained from the range gated camera available in the system. Laser ranging works on the basic time of flight (TOF) principle [28]. The time gap (δt) between transmitted pulse and received pulse gives a measure of range (R) of the target based on the following equation.

$$R = \frac{c\Delta t}{2} \tag{6}$$

where, c is velocity of the light.

Nd:YAG Laser source used for the imaging of the target in the system is used for the range measurement of the target accurately. This is done by providing an additional channel parallelly detecting reflected signals using a separate module using an APD.

Table 4 Energy/power density with beam divergence of 10 m rad at different ranges

Transmitted energy E_t (J)	Range (R) m	Energy density (J/cm^2)	Average power density (W/cm^2)
0.002	100	2.54777E-07	2.54777E-05
0.002	500	1.01911E-08	1.01911E-06
0.002	1000	2.54777E-09	2.54777E-07
0.002	1500	1.13234E-09	1.13234E-07
0.002	2000	6.36943E-10	6.36943E-08

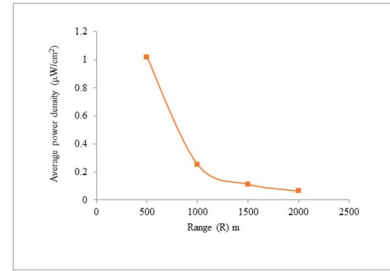


Fig. 6 Average power density as a function of range

Laser safety hazards classifications

The proposed Laser operates at the wavelength of 1064nm with pulse energy about 1–2 mJ and pulse repetition rate of 100 Hz. The pulse width of laser is ≈ 10 ns and it works with an average Laser power of 100 m W. Accordingly, this is classified as a Class 3B Laser which is not eye safe by itself. The Personnel operating the Laser at the Laser head make use of suitable Laser safety goggles to protect themselves from the potential Laser hazard. To make it eye safe for field applications a suitable beam expander with variable divergence up to 10 m rad is being used. The table below shows the Energy/power density with the beam divergence of 10 m rad at different distances in the field. Energy density and average power density are calculated for different ranges of the target. The pertinent data is shown in Table 4. Figure 6. shows average power density as a function of range. It can be seen from the above Table that operation of LIDAR in the field meets the conditions of eye safe as specified MPE as per the ANSI Z136 series of laser safety standards.

Conclusion and future scope

Design principle and analysis of an active lidar system was anticipated for security and surveillance applications operating at the wavelength 1064 nm for day and night at different adverse atmospheric conditions. The selection of components and operation of the system, especially for night

vision imaging was illustrated by a block diagram. Also, a separate channel equipped with APD detector module was proposed to measure the range of the target simultaneously. The received energy/power and SNR for different values of reflectivity and size of the target at 2 km were calculated. The factors affecting the imaging system viz., resolution, atmospheric turbulence, and atmospheric attenuation have been discussed. The use of range gating technique was described, which enables the imaging of the target at a fixed range, while eliminating the atmospheric effects. The accurate range of the target from the proposed lidar can be measured with good accuracy. The Class 3B Laser source (Nd: YAG Laser) was proposed to design the system, which is not an eye safe laser. To make it eye safe for field applications a suitable beam expander with variable divergence up to 10 m rad was proposed. The proposed design of the lidar system can be used for security and surveillance applications in defence and other security sectors. Effects of ambient atmospheric conditions on the image quality and contrast are some of the issues in the lidar imaging system. In order to reduce these effects, it is planned to conduct field experiments under different conditions of the atmosphere. Such studies are necessary to model the atmospheric effects including day and night, different sessional conditions, etc. Based on the field experiments it is proposed to use suitable AI algorithms to compensate for the atmospheric effects and improve the image quality and real time conditions when the system is operation for its application. And extending the range up to 5 Km and highly resolved images through advanced image processing algorithms could further extend its application in autonomous vehicles, drones, and robotics.

Acknowledgements The authors acknowledge the financial support from DRDO, Govt. of India under ER&IPR scheme through Project No. ERIP/ER/202108001/M/01 /1786. The authors thank Management of VNRVJIET, Hyderabad for awarding additional funding for this work.

References

- Simulation of Active Imaging Systems (Final Report of SET-219), The NATO Science and Technology Organization (2018), ISBN 978-92-837-2188-8. <https://apps.dtic.mil/sti/pdfs/AD1067687.pdf>
- S.A. Ahmed, M. Mohsin, S.M.Z. Ali, Survey and technological analysis of laser and its defense applications. *Def. Technol.* **17**, 583–592 (2021). <https://doi.org/10.1016/j.dt.2020.02.012>
- M. Xie, P. Liu, C. Ma, W. Hao, W. Huang, X. Lian, Z. Li, J. Han, Research on active polarization imaging experiments and key technologies in smoke and dust environment. *Optik* **198**, 163309 (2019). <https://doi.org/10.1016/j.ijleo.2019.163309>
- P. Sudhakar, K. Anitha Sheela, M. Satyanarayana, Imaging lidar system for night vision and surveillance applications, In Conference: advanced computing and communication systems - ICACCS 2017 (IEEE Xplore). <https://ieeexplore.ieee.org/document/8014690>
- S. Ramasamy, R. Sabatini, A. Gardi, J. Liu, LIDAR obstacle warning and avoidance system for unmanned aerial vehicle sense-and-avoid. *Aerosp. Sci. Technol.* **55**, 344–358 (2016). <https://doi.org/10.1016/j.ast.2016.05.020>
- M. Bietresato, G. Carabin, R. Vidoni, A. Gasparetto, F. Mazzetto, Evaluation of a LiDAR-based 3D-stereoscopic vision system for crop-monitoring applications. *Comput. Electron. Agric.* **124**, 1–13 (2016). <https://doi.org/10.1016/j.compag.2016.03.017>
- M. Lesser, *3-Charge coupled device (CCD) image sensors, high performance silicon, imaging fundamentals and applications of CMOS and CCD sensors* (Woodhead Publishing, Daryaganj, 2014), pp.78–97
- G. Popa, M.-A. Gheți, E. Tudor, I. Vasile, I.-C. Sburulan, Experimental study regarding long range LiDAR capabilities in sensing safety distance for vehicle application. *Sensors* **22**(15), 5731 (2022). <https://doi.org/10.3390/s22155731>
- P.Y. Jiang, Z.P. Li, W.L. Ye, Y. Hong, C. Dai, X. Huang, S.Q. Xi, J. Lu, D.J. Cui, Y. Cao, F. Xu, J.W. Pan, Long range 3D imaging through atmospheric obscurants using array-based single-photon LiDAR. *Opt. Express* **31**(10), 16054–16066 (2023). <https://doi.org/10.1364/OE.487560>. (PMID: 37157692)
- Ahui Hou, Hu. Yihua, Nanxiang Zhao, Zhenglei Dou, Xiao Dong, Xu. Shilong, Fei Han, Jiajie Fang, Advancement on target ranging and tracking by four-quadrant photon counting lidar. *Opt. Express* **32**(13), 22537–22550 (2024)
- T. Mizuno, M. Mita, Y. Kajikawa, N. Takeyama, Study of two-dimensional scanning LIDAR for planetary explorer, Proceedings of SPIE - The International Society for Optical Engineering (2008). <https://doi.org/10.1117/12.800791>
- R.K. Martin, C. Keyser, L. Ausley, M. Steinke, LADAR system and algorithm design for spectropolarimetric scene characterization. *IEEE Trans. Geosci. Remote Sens.* **56**, 3735–3746 (2018). <https://doi.org/10.1109/TGRS.2018.2809568>
- D.-L. Kim, H.-W. Park, Y.-M. Yeon, Analysis of optimal detection range performance of LiDAR systems applying coaxial optics. *Heliyon* **8**, e12493 (2022). <https://doi.org/10.1016/j.heliyon.2022.e12493>
- X. Ge, S. Chen, Y. Zhang, H. Chen, P. Guo, T. Mu, J. Yang, Telescope design for 2 μ m space based coherent wind lidar system. *Opt. Commun.* **315**, 238–242 (2014). <https://doi.org/10.1016/j.optcom.2013.11.020>
- A.S. Huntington, *3 - APD photoreceivers for range-finding and lidar, InGaAs Avalanche photodiodes for ranging and lidar* (Woodhead Publishing Series in Electronic and Optical Materials, Daryaganj, 2020). <https://doi.org/10.1016/B978-0-08-102725-7.00003-9>
- J. Sun, J. Liu, Q. Wang, A multiple-slit streak tube imaging lidar and its detection ability analysis by flash lidar equation. *Optik* **124**, 204–208 (2013). <https://doi.org/10.1016/j.ijleo.2011.11.073>
- Y. Xia, Z. Sun, A. Tok, S. Ritchie, A dense background representation method for traffic surveillance based on roadside LiDAR. *Opt. Lasers Eng.* **152**, 106982 (2022). <https://doi.org/10.1016/j.optlaseng.2022.106982>
- X. Han, H. Guo, L. Yang, L. Zhu, D. Yang, H. Xie, F. Wang, L. Chen, B. Chen, L. He, Dark current and noise analysis for Long-wavelength infrared HgCdTe avalanche photodiodes. *Infrared Phys. Technol.* **123**, 104108 (2022). <https://doi.org/10.1016/j.infrared.2022.104108>
- A. Buchner, S. Hadrath, R. Burkard, F.M. Kolb, J. Ruskowski, M. Ligges, A. Grabmaier, Analytical evaluation of signal-to-noise ratios for avalanche- and single-photon avalanche diodes. *Sensors* **21**, 2887 (2021). <https://doi.org/10.3390/s21082887>
- S. Zamek, Y. Yitzhaky, Turbulence strength cn^2 estimation from an arbitrary set of atmospherically degraded images. *J. Opt. Soc. Am. A* **23**, 3106–3113 (2006). <https://doi.org/10.1364/JOSAA.23.003106>

21. J. Liu, P. Wang, X. Zhang, Y. He, X. Zhou, H. Ye, Y. Li, S. Xu, S. Chen, D. Fan, Deep learning based atmospheric turbulence compensation for orbital angular momentum beam distortion and communication. *Opt. Express* **27**, 16671–16688 (2019). <https://doi.org/10.1364/OE.27.016671>
22. R.K. Saha, E. Salcin, J. Kim, J. Smith, S. Jayasuriya, *Turbulence strength estimation from video using physics-based deep learning* (Optica Publishing Group, Washington, 2022). <https://doi.org/10.1364/OE.469976>
23. Lu. Tian-an, Hong-ping Li, Atmospheric turbulence induced synthetic aperture lidar phase error compensation. *Opt. Commun.* **381**, 214–221 (2016). <https://doi.org/10.1016/j.optcom.2016.06.089>
24. Z. Tian, G. Yang, Y. Zhang, Z. Cui, Z. Bi, A range-gated imaging flash Lidar based on the adjacent frame difference method. *Opt. Lasers Eng.* **141**, 106558 (2021). <https://doi.org/10.1016/j.optlaseng.2021.106558>
25. S. Wang, S. Tao, D. Chen, G. Gu, Improved long distance range-gated laser imaging system. *Optoelectron. Lett.* **15**, 21–25 (2019). <https://doi.org/10.1007/s11801-019-8077-6>
26. Z. Li, C. Jiang, X. Gu, Y. Xu, F. Zhou, J. Cui, Collaborative positioning for swarms: a brief survey of vision, LiDAR and wireless sensors-based methods. *Def. Technol.* (2024). <https://doi.org/10.1016/j.dt.2023.05.013>
27. H. Rahman, G.C. Paul, Tripartite sub-image histogram equalization for slightly low contrast gray-tone image enhancement. *Pattern Recognit.* **134**, 109043 (2023). <https://doi.org/10.1016/j.patcog.2022.109043>
28. S. Kruapech, J. Widjaja, Laser range finder using Gaussian beam range equation. *Opt. Laser Technol.* **42**, 749–754 (2010). <https://doi.org/10.1016/j.optlastec.2009.11.020>

Publisher's Note Springer Nature remains neutral with regard to jurisdictional claims in published maps and institutional affiliations.

Springer Nature or its licensor (e.g. a society or other partner) holds exclusive rights to this article under a publishing agreement with the author(s) or other rightsholder(s); author self-archiving of the accepted manuscript version of this article is solely governed by the terms of such publishing agreement and applicable law.